Relativistic, retardation, and multipole effects in photoionization cross sections: Z, n, and l dependence

Akiva Ron, I. B. Goldberg, and J. Stein
Racah Institute of Physics, The Hebrew University of Jerusalem, Jerusalem 91904, Israel

Steven T. Manson
Department of Physics and Astronomy, Georgia State University, Atlanta, Georgia 30303

R. H. Pratt and R. Y. Yin
Department of Physics and Astronomy, University of Pittsburgh, Pittsburgh, Pennsylvania 15260
(Received 29 September 1993)

The limits of validity of the nonrelativistic dipole formulation of the total photoionization cross section are explored. Relativistic and nonrelativistic independent particle model calculations of all subshells of C, Sn, and U are performed from 0 to 200 keV above threshold in each case. The comparison shows a remarkable agreement between nonrelativistic dipole and full relativistic multipole results for s subshells, even at the highest energies investigated where nonrelativistic dipole approximation should show significant breakdown; this phenomenon does not occur for $l \neq 0$ subshells or in angular distributions. The phenomenon is explained in terms of an approximate cancellation among relativistic, retardation, and multipole effects which occurs only for s subshells.

PACS number(s): 32.80.Fb

I. INTRODUCTION

The response of an atom to the absorption of electromagnetic radiation, the process of photoionization, is of interest as it is one of the most fundamental processes in nature. In addition, photoionization is of interest owing to its importance in various applications. A number of reviews exist which survey the field for low photon energies and low Z, where relativistic effects are relatively unimportant, but many-electron correlations can be significant [1,2], along with a review of high-energy photoionization, where the various effects of relativistic interactions are quite important while correlation can generally be neglected [3]. Certainly a fully relativistic multipole (FM) calculation will work quite well for low energy and low Z, but such a calculation requires considerably more effort than the much simpler nonrelativistic nonretarded dipole (ND) approximation, which is generally employed at low energy. Since the nonrelativistic dipole calculation is so much simpler than the fully relativistic calculation, it is of interest to determine its limits of validity in some detail.

It was noted some time ago [4] that nonrelativistic dipole total cross sections (but not angular distributions) for the photoelectric effect of s states are valid far beyond their anticipated energy limits. This was noted for bremsstrahlung and internal conversion as well [5,6]. More recent applications have also included direct radiative recombination and photon-atom scattering [7–10]. In this paper we explore the validity of the nonrelativistic dipole approximation for total photoionization cross sections by performing such calculations over a broad range of energy Z and subshells and comparing with our calculations using a fully relativistic multipole formulation. In particular, calculations are performed for all subshells of C ($Z=6$), Sn ($Z=50$), and U ($Z=92$), from threshold to 200 keV above threshold for each subshell. For simplicity, the independent-particle approximation, which neglects electron correlation and approximates exchange, is utilized. Since we are interested predominantly in high energies, well above threshold, it is not expected that the use of such an approximation significantly affects conclusions concerning the importance of relativistic, retardation, and multipole effects.

In addition to delineating the limits of validity of the nonrelativistic dipole approximation, we have also attempted to discern which aspect(s) of the fully relativistic multipole (FM) calculation are responsible for the breakdown in a given case. To this end we classify additional features of the FM calculation [3] as relativistic effects, by which we mean the relativistic modifications of potentials, wave functions, energies, and transition operators; retardation effects in the transition operator; and multipole effects in the transition operator.

In Sec. II, we present a brief review of the various relativistic and nonrelativistic calculations performed, from the FM to the ND, along with the atomic models employed and a detailed definition of the relativistic, retardation, and multipole effects mentioned above. Section III presents and discusses a detailed comparison of all of our ND and FM results, while Sec. IV attempts to explain these results in terms of the various relativistic, retardation, and multipole interactions. Finally, a summary and conclusion are presented in Sec. V.

II. BRIEF REVIEW OF THEORY

A. Common features of nonrelativistic and relativistic calculations

All calculations reported herein are performed within the framework of independent-particle wave functions.

The range of energies we considered is such that correlation and exchange effects do not generally contribute appreciably to photoionization cross sections many keV above threshold, as is well known [1]. The atomic potentials are obtained self-consistently using the central-field Slater approximation to exchange with the Latter tail to remove the self-interaction. This approximation is generally referred to as the Hartree-Slater (HS) approximation [11] in the nonrelativistic case, and the Dirac-Slater (DS) approximation in the relativistic case [12].

The similarity of ND and FM total cross sections was first noted for $L1$- and K-shell photoionization [4]. In this paper, we investigate the dependence of this effect on the principal quantum number n, initial state angular momentum l, photoelectron energy from threshold to 200 keV, and atomic number Z ($Z=6$, 50, and 92) in an effort to determine the limitations and causes of this effect.

The nonrelativistic interaction between the radiation field and the electron momentum in Coulomb gauge is proportional to $\exp(i\mathbf{k}\cdot\mathbf{r})\mathbf{p}$, where $\mathbf{p}$ is the electron momentum operator and $\mathbf{k}$ is the photon wave number, while the relativistic interaction is proportional to $\exp(i\mathbf{k}\cdot\mathbf{r})\boldsymbol{\alpha}$, where the components of $\boldsymbol{\alpha}$ are the 4×4 Dirac matrices. To perform the calculations, these interactions are expanded in a series of products of vector spherical harmonics and spherical Bessel functions [13] known as a multipole expansion [3]. To make the (electric) dipole approximation means to truncate the series and consider only the odd-parity portion of the $L=1$ term in the expansion while preserving the full spherical Bessel functions. Neglect of the retardation means replacing the spherical Bessel function $j_0(kr)$ by unity and $j_2(kr)$ by zero in the dipole term; the (electric) dipole approximation with no retardation is equivalent to setting $\exp(i\mathbf{k}\cdot\mathbf{r})$, which appears in the matrix element, to unity. It is thus clear that, in general, neglect of the retardation is not the same thing as the electric dipole approximation. Both approximations start to break down as the photon energy becomes large enough so that $\mathbf{k}\cdot\mathbf{r}$ is no longer small. Owing to the range of values of r which contribute to the matrix element, it is found that the validity of such approximations breaks down for all atomic subshells for photon energies higher than about 20 keV [3].

B. Nature of the nonrelativistic calculation

The cross section for photoionization is proportional to the square of the matrix element [2,14]

$$|\langle\psi_f|\exp(i\mathbf{k}\cdot\mathbf{r})\mathbf{p}\cdot\boldsymbol{\epsilon}|\psi_i\rangle|^2 , \tag{1}$$

where ψ_i and ψ_f, the initial (bound) and final (continuum) wave functions, are solutions of Schrödinger's equation in the self-consistent-field Hartree-Slater potential [11], and $\boldsymbol{\epsilon}$ is the polarization vector of the photon. The interaction is expanded into a series of multipoles as described above. However when $\mathbf{k}\cdot\mathbf{r}>1$ there can be a big deviation from the "no retardation" result even if the series is truncated so that only the dipole term is retained. As mentioned above, this will happen for photon energies higher than about 20 keV.

C. Nature of the relativistic calculation

In this case, the photoionization cross sections are proportional to [3,13,15]

$$|\langle\psi_f|\exp(i\mathbf{k}\cdot\mathbf{r})\boldsymbol{\alpha}\cdot\boldsymbol{\epsilon}|\psi_i\rangle|^2 , \tag{2}$$

where ψ_i and ψ_f are solutions of Dirac's equation with the self-consistent-field electrostatic potential of Lieberman [12]. The final continuum wave functions are given in a partial wave expansion to all orders, and the total cross section is computed for any number of multipoles desired [16].

D. Retardation, multipole and relativistic effects

As described above, calculations can be performed which vary in different particulars: The use of Dirac's vs Schrödinger's equation to obtain wave functions along with the use of relativistic vs nonrelativistic transition operators; the use of dipole vs multipole expansions; and the use of "no retardation" vs retardation approximations. If we could examine the influence of each of these separate effects unambiguously, we would be able to check the assertion that some cancellation among them is the reason for the phenomenon observed. In order to investigate the interlay of these various effects, we have calculated six sets of cross sections. Set I, nonrelativistic, dipole, no retardation; set II, nonrelativistic, dipole, with retardation; set III, nonrelativistic, multipole, with retardation; set IV, relativistic, dipole, no retardation; set V, relativistic, dipole, with retardation; set VI, relativistic, multipole, with retardation. The ND and FM calculations described in former subsections are sets I and VI, respectively.

The relativistic calculations were carried out using our own codes [17]. Our relativistic formalism uses a partial wave expansion for the continuum wave function, the multipole expansion for the interaction of electromagnetic field, and the electron current to perform the FM calculations. However, the codes are flexible enough to allow us to "turn off" the higher multipoles, to achieve set-V calculations, and "turn off" retardation as well, which gives set-IV results. One can also achieve nonrelativistic results from these codes, by the following procedure: We let the speed of light c tend toward infinity in the expressions

$$\lambda_C=\frac{\hbar}{mc},\quad \alpha=\frac{e^2}{\hbar c},\quad \epsilon=1+\frac{E}{mc^2} ,$$

whenever they appear in the potential and photoionization codes (which solve Dirac's equation for both the bound and continuum functions), except for the photon wave number $|\mathbf{k}|=\omega/c$, which appears in the transition operators Eqs. (1) and (2). The results obtained by this procedure are the set-III results, the nonrelativistic limit of set VI. If we allow c to tend toward infinity in the expression for $\mathbf{k}$ as well, we obtain the long-wavelength limit of the nonrelativistic results in which the higher multipoles and retardation are omitted, i.e., set I. To check the numerical accuracy of this technique, we performed ND calculations and reproduced the results obtained

with an independent nonrelativistic code [18] to an accuracy of 4–5 significant digits. This comparison also confirmed that the relativistic DS potential approaches the nonrelativistic HS in that limit [19].

It was pointed out in Sec. II A that multipole and retardation effects would be expected to be noticeable in the total cross section at photon energies higher than about 20 keV for any atomic subshell. Since the ND formalism neglects retardation and higher multipoles, one should detect differences between ND and FM results in the range of tens of keV. As for relativistic effects, the parameter

$$\gamma = \frac{1}{\sqrt{1-\beta^2}}$$

can serve as an indicator of the extent of being in the relativistic domain. For electron kinetic energies of 20 and 200 keV, we find that γ is 1.04 and 1.40, respectively (γ is 2 for an electron energy of 511 keV). If this parameter can be taken as an estimate of differences between relativistic and nonrelativistic results, then we expect significant increases in the differences in going from 20 to 200 keV.

III. COMPARISON OF NONRELATIVISTIC DIPOLE (ND) AND FULLY RELATIVISTIC MULTIPOLE (FM) RESULTS

As described in Sec. II, we can classify the effects of interactions included in the FM calculation as (1) relativistic effects on the potential, and the initial discrete and final state wave functions, energies, and transition operators; (2) the effects of higher multipoles; and (3) the effects of retardation. The FM calculation contains all three effects, while the ND includes none of them. Here we examine the ratio FM/ND for all of the cases calculated.

The ratios presented in Figs. 1–3 are for

$$(\sigma_{l,j=l-1/2}+\sigma_{l,j=l+1/2})_{\rm rel}/(\sigma_l)_{\rm ND}\ .$$

We use these ratios because in the ND case we do not have the splitting of the subshells into two states. Furthermore, the cancellation phenomenon occurs in the s states which do not have this splitting. We will address the problem of this spin dependence later in this section. In each of the figures presented, the ratios for a number of different subshells are shown. Therefore, for clarity, the ratios are given as functions of the continuum electron energy [20].

In Fig. 1, this ratio is shown for C 1s, 2s, and 2p over the range from 0 to 200 keV above threshold. Near threshold, the ratios are essentially unity, which indicates that ND is adequate there (which, of course, we already knew). With increasing photoelectron energy, however, the 2p ratio increases rapidly to about 2.20 at 200 keV, while the 1s and 2s ratios increase only very slightly and lie essentially on the same curve; they reach a value of about 1.16 at 200 keV. In other words, at 200 keV $\sigma_{\rm FM}$ is about 16% larger than $\sigma_{\rm ND}$ for C 1s and 2s, but 120% larger for 2p, indicating that the ND total cross section calculation remains valid for C 1s and 2s to much higher energies than it does for 2p.

To check the generality of these results, the situation for Sn is shown in Fig. 2, where a similar, but more complex, picture is evident. Nevertheless, it is clear that the results for Sn are grouped by the angular momentum of the initial states. For initial s states in Sn, the ratio increases from near unity at threshold to 1.16–1.24 (depending on principal quantum number n) at 200 keV. The curves form two groups: the 1s shell, which is a deep inner shell with a binding energy almost 30 keV; and the 2s, 3s, and 4s subshells, which are intermediate inner shells, and the 5s subshell which contains valence electrons. The 1s inner subshell changes the least with increasing energy, while the valence 5s ratio changes the most. Still the ratios are similar to s-state ratios in carbon.

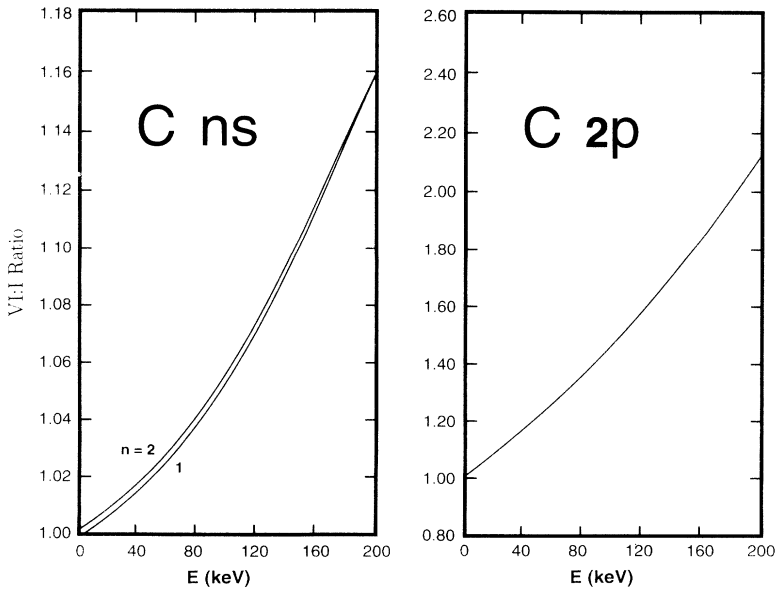

FIG. 1. Ratios of the fully relativistic multipole (FM) photoionization cross sections (VI) to the nonrelativistic dipole (ND) results (I) for (a) C ns (left) and (b) C 2p (right) subshells as a function of photoelectron energy E.

For p states in Sn, the ratios are all seen to lie along the same curve, which increases from near unity at the threshold to 2.30 at 200 keV, a situation almost exactly like the case of C $2p$, and much different from the s states. Furthermore, the Sn $3d$ and $4d$ ratios lie along the same curve, which increases from near unity at threshold to 3.20 at 200 keV. It thus appears that the ND treatment of photoionization becomes much worse at higher energies with increasing initial-state angular momentum.

The situation remains similar for photoionization of U, depicted in Fig. 3. For ns states in U, the ratio increases from near unity at threshold to a range 1.25–1.50 at 200 keV, with the ratio lowest for $1s$ and highest for $7s$. As in Sn, the ratios split into groups with the $1s$ result, whose binding energy is more than 100 keV, by itself; the $2s$, $3s$, $4s$, and $5s$ (in intermediate inner subshells) on nearly the same curve; and the near-valence $6s$ and outermost $7s$ ratios each lying along their own curves. The s-subshell ratios for U are a bit higher than for C or Sn, indicating that there are additional physical effects which are important for photoionization of U, but not important in C or Sn s-subshell photoionization.

The p-subshell cross-section ratios, unlike the case of Sn, split into two groups: the $2p$ case, which is bound by

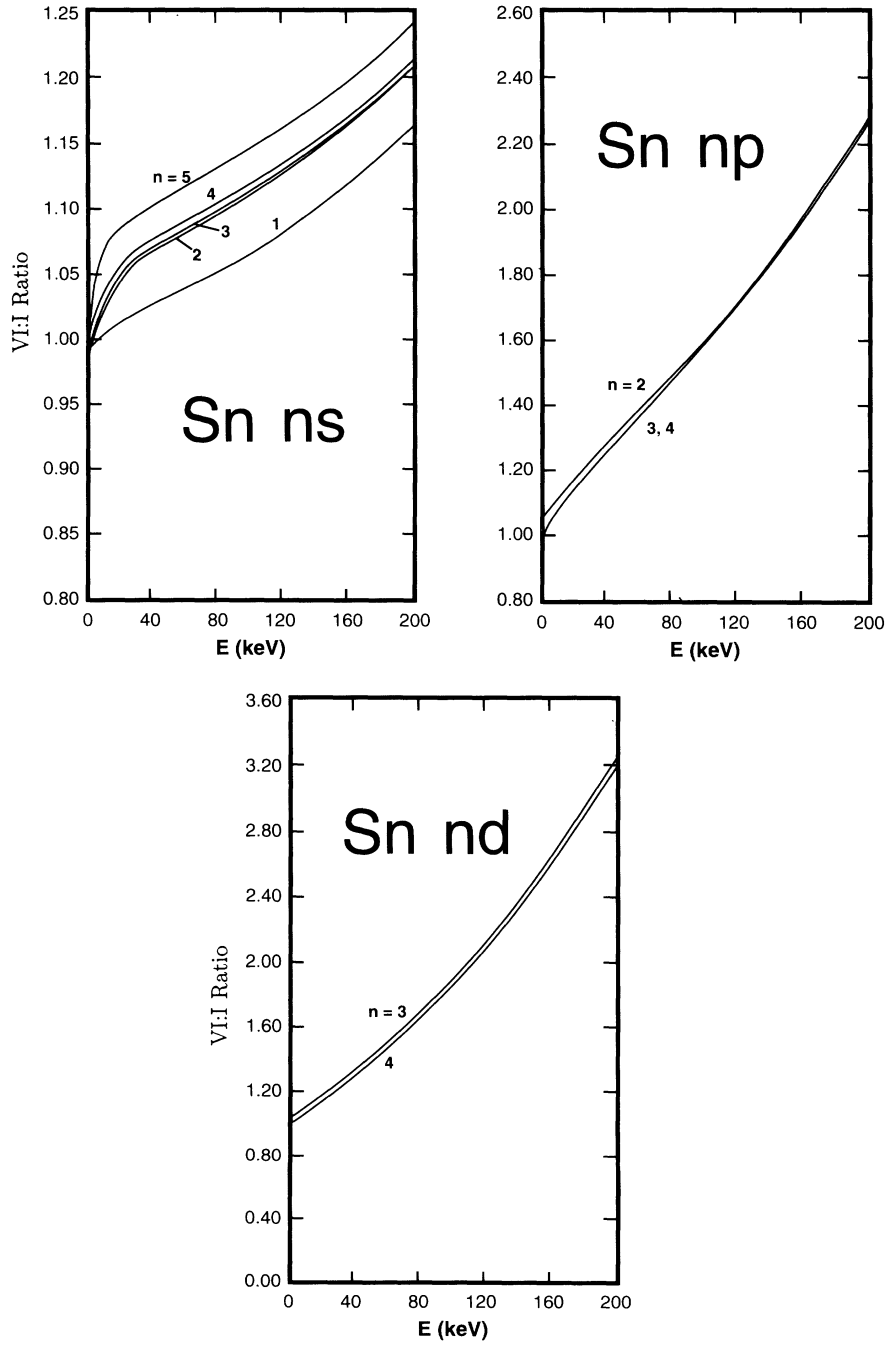

FIG. 2. As Fig. 1, but for (a) Sn ns (upper left), (b) Sn np (upper right), and (c) Sn nd (below) subshells.

about 15 keV, is highest, going to a ratio of about 3.20 at 200 keV; while the other (less tightly bound) p-state ratios are about 3.0 at 200 keV. All of these p-subshell ratios in U approach significantly larger values, at the higher energies, than the p-state ratios in Sn or C. Again, this indicates that additional physical effects are more important in U than in C and Sn.

The ratios for d's are split into two distinct groups, again unlike Sn. But unlike the p-state ratios, it is the valence $6d$ ratio that is split off and goes to 2.60 at 200 keV; the $3d$, $4d$, and $5d$ are quite close together and approach about 3.25 at 200 keV. Note that the 200-keV ratios are about the same for p- and d-subshell photoionization in U, as opposed to Sn, where the high-energy ratio is considerably larger for the d states.

For the $4f$ and $5f$ states in U, the curves are slightly separated, with $5f$ being lower, and they go to ratios of about 4.60 and 3.90, respectively, at 200 keV. Thus for U, as for Sn and C, for s-state photoionization, even for photoelectron energies of 200 keV, the FM and ND results are remarkably similar, while for $l \neq 0$ the results differ by factors of 3 or more.

Up to this point we have compared ratios of cross sections of complete subshells, i.e., $(\sigma_{2p_{1/2}}+\sigma_{2p_{3/2}})/\sigma_{2p}^{\mathrm{ND}}$ and disregarded the j dependence. We can define $\Sigma_{nlj}^{\mathrm{FM}}$ and $\Sigma_{nl}^{\mathrm{ND}}$ as cross sections per electron and look at the ra-

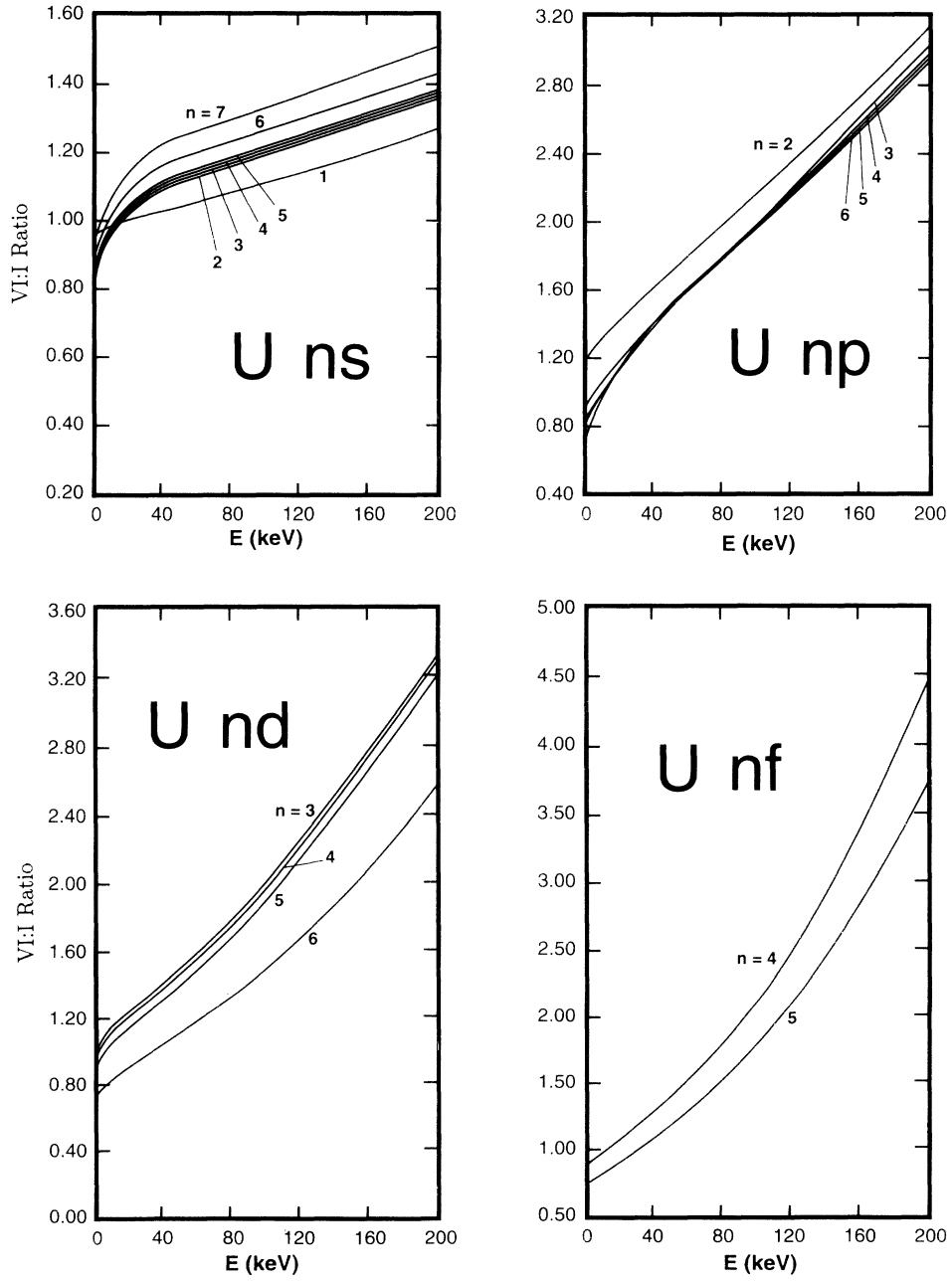

FIG. 3. As Fig. 1, but for (a) U ns (upper left), (b) U np (upper right), (c) U nd (lower left), and (d) U nf (lower right) subshells.

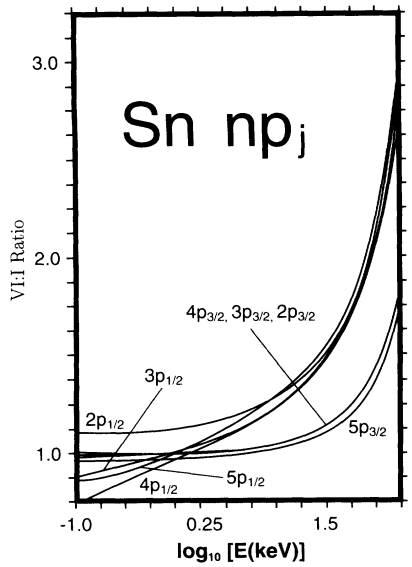

FIG. 4. As Fig. 1 for the Sn np_j subshells. Note that the horizontal scale is logarithmic.

tios $\Sigma^{FM}_{nlj=l\pm1/2}/\Sigma^{ND}_{nl}$. We observe that somewhat away from thresholds the ratios for $j=l_{-1/2}$ are larger than the ratios for $j=l_{+1/2}$. We present an example of this behavior in Fig. 4, which shows the behavior of p states in Sn. All $np_{1/2}$ ratios are larger than those of $np_{3/2}$ states, except close to threshold. This behavior also is found for d and f states of Sn and for C and U.

IV. DISCUSSION OF OTHER RESULTS

In Sec. II B we defined and described various types of calculations which generated cross sections which we denoted as sets I–VI. The ratios of cross sections of two different sets (for a given subshell and the same photon energies) give an idea of the relative importance of a certain effect because each set of calculations includes some effects but omits others. In Sec. III we discussed the VI:I ratio, where VI is the FM including all effects (relativistic, multipole, and retardation) and I is ND and includes none. Thus we discussed the overall effect. In the same spirit we may expect that the VI:V and III:II ratios will suggest the influences of multipole effects, the V:IV and II:I ratios will reflect the influence of retardation and the IV:I, V:II, and VI:III ratios will give an idea of relativistic effects. Were the different effects strictly separable, then all ratios within a given group would be the same and the conclusions unequivocal. In practice the different ratios within a group are not identical. Probably this reflects diverse patterns of "interference" among the different effects. To the extend that somewhat different conclusions can be reached by examining different ratios of sets which may be expected to reflect the influence of the same effect, one cannot make definitive statements as to the individual role of each of these effects. We present one set of ratios from each group—IV:I, V:IV, and III:II—as examples of each effect. Before looking at the above ratios in detail, it is of interest to obtain some idea of how the ratios in each group compare with each other. Basically, the results show that for ns photoionization, differing ratios within each group are in agreement; deviations not larger than about 10% are found even as high as 200 keV above threshold. For other cases, deviations as large as a factor of 2 are found. This emphasizes that the separation of the various effects is not unique, in general, but close to unique for s states. With this caveat in mind, we proceed to a discussion of the ratios.

Figure 5(a) shows the IV:I ratios as functions of energy for the ns states of Sn, which highlight the influence of the relativistic effect. The ratios start near unity in the low-energy range, then drop very quickly to 0.60–0.65 as energy increases; the higher the principal quantum number n, the larger is the ratio. In fact, we find a similar behavior for s and p states of carbon and also for p and d states of tin, except that the curves are more merged and go down to 0.55–0.82, depending on the value of l. However, the behavior is not monotonic as a function of l or n; the n dependence for $l\neq0$ states is not monotonic as in the $l=0$ case. Still Fig. 5(a) is a typical representation of relativistic effects. Our conclusion for this point is that

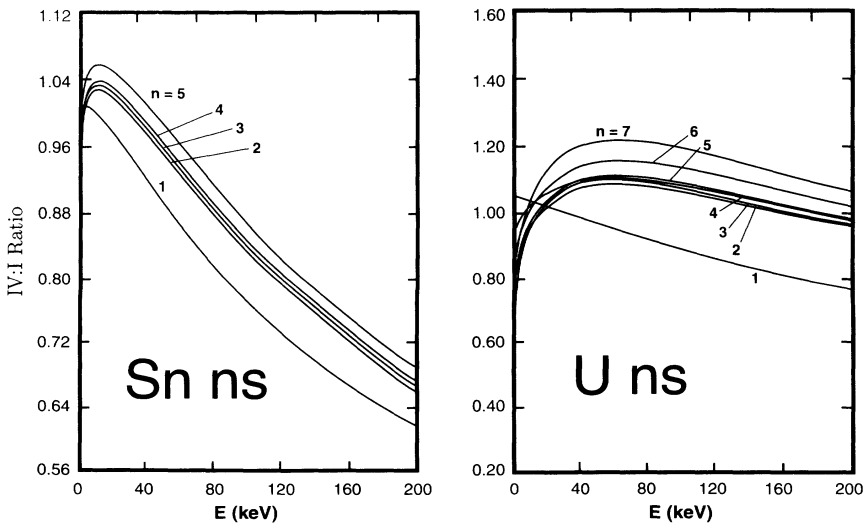

FIG. 5. Ratios of the relativistic dipole without retardation photoionization cross sections (IV) to the nonrelativistic dipole without retardation (ND) results (I) for (a) Sn ns (left) and (b) U ns (right) subshells as a function of photoelectron energy E.

relativistic effects reduce the ND cross sections for photoelectron energies well above threshold. When we examine the IV:I ratios of uranium for d and f states we encounter the same behavior as described for carbon and tin. However, the s and p states show a different picture; looking at Fig. 5(b) for uranium s states, one sees that at lower energies the ratios go up to about 1.05–1.20 (the higher n, the larger the ratio) and then begin to drop, to about 0.95–1.05, except for the $1s$ ratio which behaves as in carbon and tin. The behavior of the p states is very similar and even exhibits the same n dependence as the s states. The only difference is in the magnitude; the ratios go up to about 1.40 and then drop at 1.25–1.35 depending on n. Thus it is clear that relativistic effects, which include relativistic effects on initial- and final-state wave functions, along with the transition operator, cause rather different results in a very heavy atom (U) as opposed to intermediate (Sn) or light (C) atoms.

The second type of ratio, V:IV, indicates the retardation effect. They are shown for p states of tin in Fig. 6(a) as a function of photoelectron energy. These ratios increase from 1 to about 1.2, and all curves merge into one curve. This behavior is typical for all other subshells except for the s subshells of tin and uranium. The different behavior of the s subshells of the high-Z elements is shown in Fig. 6(b), where the ratios of uranium s subshells are plotted. These start at about 1, rise slightly, and then decrease to about 1 again at high energy. The $2s$ ratio has the same shape as the higher subshell ratios but is smaller, about 0.98 vs 1.01; the $1s$ has a different shape and monotonically increases from 0.88 to 0.91. Figure 6(c) shows the same for Sn. Here we have only the

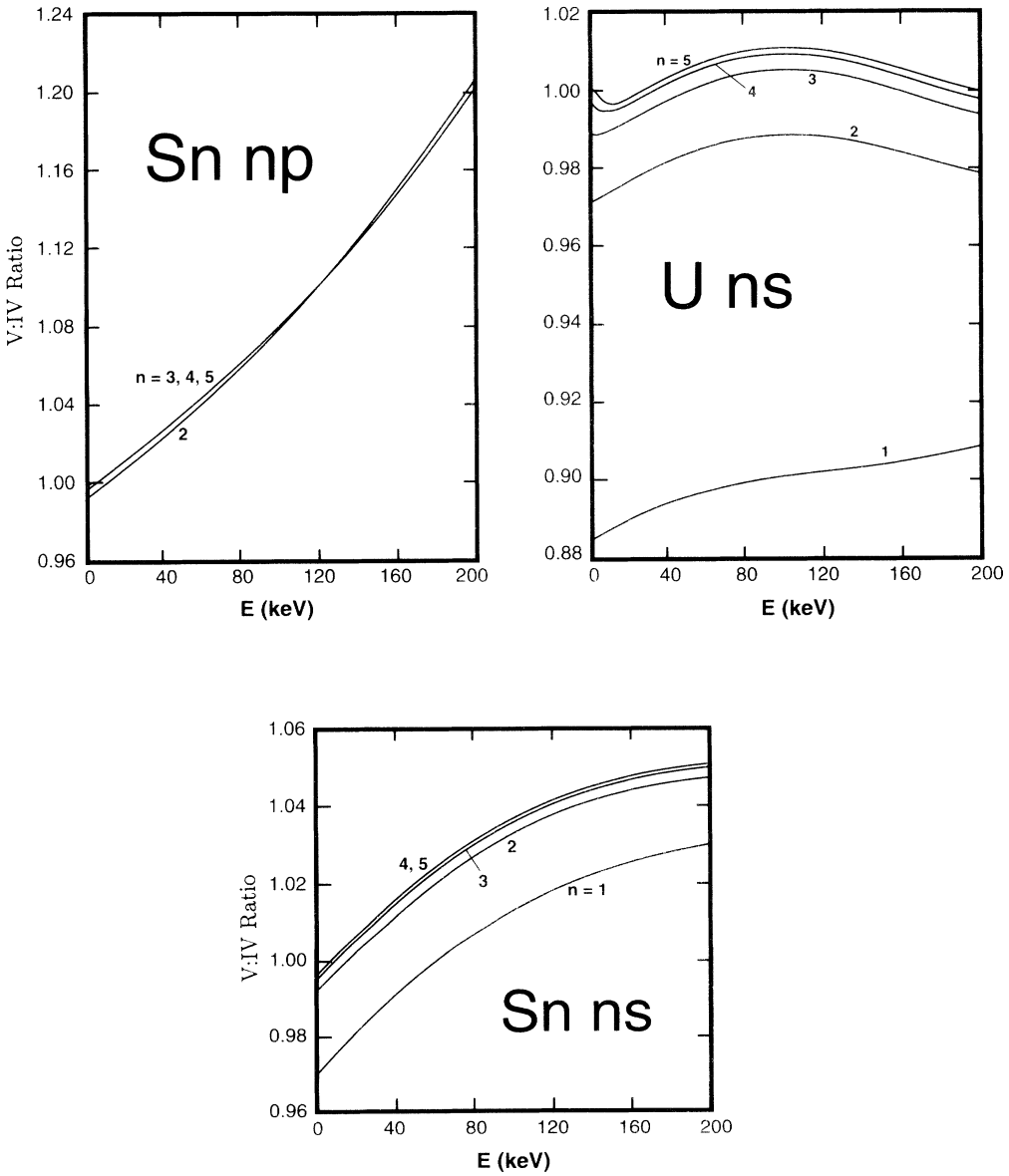

FIG. 6. Ratios of the relativistic dipole with retardation photoionization cross sections (V) to the relativistic dipole without retardation results (IV) for (a) Sn np (upper left), (b) U ns (upper right), and (c) Sn ns (below) subshells as a function of photoelectron energy E.

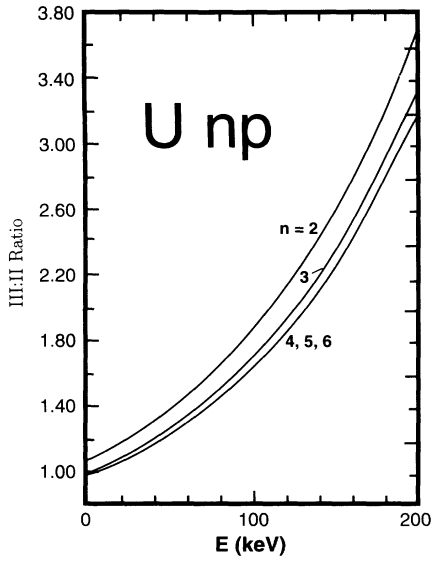

FIG. 7. Ratios of the nonrelativistic multipole with retardation photoionization cross sections (III) to the nonrelativistic dipole with retardation results (II) for U *np* subshells as a function of photoelectron energy *E*.

rising part of the curve, from about 1 to 1.05. One notes that these differences, due to retardation, range up to 5% for *s* states and to about 20% for other values of angular momentum.

The multipole effect on cross sections is shown in Fig. 7, illustrating the III:II *np* ratios for U. For all *n* the ratio starts at 1 (at the low-energy end), increases with energy to about 2 for *s* states, and increases with increasing *l* to 22 for *f* states at 200 keV. For a given value of *l* the curves are better merged for lower values of *Z*. There are no exceptions to the general behavior shown in Fig. 7 as a function of *l* and *Z*. The *s*-state ratios have a similar shape but increase less rapidly, going to 2.0 for 1*s* and to 1.7 for higher *ns* states.

From these results, the general nature of the cancellation among relativistic, retardation, and multipole effects is clear. The relativistic effect *decreases* *s*-shell cross sections considerably, with increasing energy, thus partially canceling out the increase due to retardation and multipole effects; in addition, the multipole effect increases the cross section for $l \neq 0$ states much more rapidly. The combination yields the cancellation observed, which is fairly complete for *s*-state photoionization.

V. CONCLUSION

This study of ratios of relativistic and nonrelativistic photoionization calculations allows some assessment of the importance of various effects. We have found the following features.

(1) The difference between the fully relativistic multipole (FM) calculation and the nonrelativistic dipole (ND) calculation of total photoelectric cross sections is much less pronounced for *s* states ($l=0$) than for $l>0$. The FM-to-ND cross section ratio at 200 keV above threshold increases with the atomic number *Z* from 1.16 for C to 1.50 for U, for *s* states. The ratios at 200 keV also increase by a factor 2–3 over those of *s* states with increasing angular momentum *l*.

(2) Ratios, as a function of energy, tend to merge to a common curve with increasing principal quantum number *n*. For $l>0$, the higher ratios are obtained for lower values of *n*. For $l=0$ it is the opposite, the lower the value of *n* the lower are the ratios; in addition, the curves are more separated.

(3) The FM-to-ND ratios of cross sections from the $j=l-\frac{1}{2}$ levels are larger than those for the $j=l+\frac{1}{2}$ levels.

(4) In general, and particularly for the highest energy that we considered, the ratios for the multipole and retardation effects are larger than 1. In particular, the ratios for the multipole effect of the *f* shell of U go up as high as 22. The ratios for the relativistic (Pauli-Schrödinger vs Dirac) effect are less than unity with one exception: for *s* states of U the ratios are growing and reach a value of 1.10–1.20 at about $E=40$–60 keV, and then go down to about 0.70.

(5) Within a group of ratios, which should describe the same effect, there may be differences not only in magnitude but in shape. Ratios within a group vary by no more than about 10% for *s* states, but the deviations are significantly larger for $l>0$ states. These deviations are more pronounced for the multipole and relativistic effects than for the retardation effect, and they increase with increasing photoelectron kinetic energy and initial angular momentum.

The uniqueness of the behavior of *s* states is twofold: Not only are *s*-state ratios lower by a factor of 2–3 [see (1) above], but they also show changes in patterns of behavior, e.g., relativistic effects [see (4) above]. These behaviors imply cancellations among the various effects, although details of the cancellations differ depending on which ratios we look at.

In any case, we have shown that nonrelativistic dipole calculations for total photoionization cross sections of *s* states have validity in energy regions well above those in which the individual approximations employed are valid, owing to cancellations between various manifestations of relativistic, retardation, and multipole interactions. This cancellation does not appear for $l \neq 0$.

ACKNOWLEDGMENT

This work was supported by the National Science Foundation under Grant Nos. PHY-9005763 and PHY-9107539.

[1] A. F. Starace, in *Handbuch der Physik*, edited by W. Mehlhorn (Springer-Verlag, Berlin, 1979), Vol. 31, pp. 1–121, and references therein.
[2] J. Berkowitz, *Photoabsorption, Photoionization, and Photoelectron Spectroscopy* (Academic, New York, 1979), and references therein.
[3] R. H. Pratt, A. Ron, and H. K. Tseng, Rev. Mod. Phys. **45**, 273 (1973).
[4] S. D. Oh, J. McEnnen, and R. H. Pratt, Phys. Rev. A **14**, 1428 (1976); for angular distributions, see A. Ron, R. H. Pratt, and H. K. Tseng, Chem. Phys. Lett. **47**, 377 (1977).
[5] S. D. Oh and R. H. Pratt, Phys. Rev. A **13**, 1463 (1976).
[6] C. M. Lee, L. Kissel, R. H. Pratt, and H. K. Tseng, Phys. Rev. A **13**, 1714 (1976).
[7] S. C. Roy and R. H. Pratt, Phys. Rev. A **26**, 651 (1982).
[8] R. H. Pratt in *X-Ray and Atomic Inner-Shell Physics—1982,* edited by B. Crasemann (Americal Institute of Physics, New York, 1982), pp. 346–356.
[9] F. D. Aaron, A. Costescu, and C. Dinu, J. Phys. (Paris) II **3**, 1227 (1993).
[10] R. H. Pratt and Y. S. Kim in *Topics in Atomic and Nuclear Collisions,* edited by B. Remaud, A. Colboreanu, and V. Zoran (Plenum, New York, in press).
[11] F. Herman and S. Skillman, *Atomic Structure Calculations* (Prentice-Hall, Englewood Cliffs, NJ, 1963).
[12] D. Lieberman, D. T. Cromer, and J. T. Waber, Comput. Phys. Commun. **2**, 107 (1971).
[13] I. P. Grant, J. Phys. B **7**, 1458 (1974).
[14] H. A. Bethe and E. S. Salpeter, *Quantum Mechanics of One- and Two-Electron Systems* (Springer-Verlag, Berlin, 1958), p. 247ff.
[15] G. Rakavy and A. Ron, Phys. Rev. **159**, 50 (1967).
[16] K.-N. Huang, Phys. Rev. A **22**, 223 (1980).
[17] I. B. Goldberg and P. M. Bergstrom Jr., University of Pittsburgh Report Pitt-387 (unpublished). See Refs. 3, 15, and 16 for earlier formulations of this calculation.
[18] S. T. Manson and J. W. Cooper, Phys. Rev. **165**, 126 (1968).
[19] It should be noted that, technically speaking, in the limiting procedure which we have described there still remains a spin dependence in the nonrelativistic results; under the action of $c \rightarrow \infty$, the Dirac equation reduces to the Pauli-Schrödinger equation. Since we are using central potentials, however, the only effect of this spin dependence for set I is to separate the $l \neq 0$ subshell cross sections into cross sections for each of the two distinct values of the total angular momentum j of each electron which differ *only* by statistical weight. The set I total subshell cross section is entirely unaffected by this spin dependence, as evidenced by the accuracy of the comparison with results based upon the Schrödinger equation.
[20] In fact, each ratio involves three (or two, for s states) bound states: two (or one) relativistic bound states ($j = l - \frac{1}{2}$ and $j = l + \frac{1}{2}$) and one nonrelativistic. The ratios were calculated at the same photon energy for each state. The results are plotted vs the photoelectron energy appropriate to the $j = l + \frac{1}{2}$ state, so that all curves begin at close to the same (zero) energy. Since the threshold region is not our primary interest, this causes no difficulty.